

Lawrence Berkeley National Laboratory

Recent Work

Title

Control of the heavy-ion beam line gas pressure and density in the HYLIFE thick-liquid chamber

Permalink

<https://escholarship.org/uc/item/9077p58c>

Journal

Fusion Energy and Design, 63-64

Authors

Debonnel, Christophe D.
Fukuda, Grant T.
Bardet, Philippe M.
et al.

Publication Date

2002-02-26



ELSEVIER

Fusion Engineering and Design 00 (2002) 1–6

**Fusion
Engineering
and Design**

www.elsevier.com/locate/fusengdes

Control of the heavy-ion beam line gas pressure and density in the HYLIFE thick-liquid chamber

Christophe S. Debonnel*, Grant T. Fukuda, Philippe M. Bardet, Per F. Peterson

Department of Nuclear Engineering, University of California at Berkeley, 4118 Etcheverry Hall, Berkeley, CA 94720, USA

Abstract

Controlling the density and pressure of the background gas in the beam lines of thick-liquid heavy-ion fusion chambers is of paramount importance for the beams to focus and propagate properly. Additionally, transport and deposition of debris material onto metal beam-tube surfaces may reduce the breakdown voltage and permit arcing with the beam. The strategy to control the gas pressure and the rate of debris deposition is twofold. First, the cool thick-liquid jet structures will mitigate the venting to the beam tubes. The ablation and venting of debris through thick-liquid structures must be modelled to predict the quantities of debris reaching the beam ports. TSUNAMI calculations have been performed to estimate the mass and energy flux histories at the entrance of the beam ports in a 9×9 HYLIFE pocket geometry. Secondly, additional renewable shielding will be interposed in the beam tubes themselves. Thick-liquid vortexes are planned to coat the inside of the beam tubes and provide a quasi-continuous protection of the beam-tube walls up to the final focus magnets. A three-component molten salt, flinabe, with a low melting temperature and vapor pressure, has been identified as a candidate liquid for the vortexes. The use of flinabe may actually eliminate the necessity of mechanical shutters to rapidly close the beam tubes after target ignition. © 2002 Published by Elsevier Science B.V.

Keywords: Heavy-ion; Gas pressure; Chamber

1. Introduction

Keeping the pressure and density low in the final-focus magnet region of heavy-ion fusion beam lines is very important for the beams to propagate and focus properly. Any stripping of ions by collisions with background gas, prior to or

in the final focus magnet region, causes the ions to be lost. Beyond the final focus magnets, the gas density can climb to the chamber value, but the density distribution and preionization of the gas must be controlled to optimize the beam neutralization and focusing performance. Estimates of the mass flux, pressure and temperature of the debris at the entrance of the beam tubes provide the inlet boundary conditions to determine the amount of debris that must be managed in the beam tubes and diverted from depositing in the final-focus magnet region. Assessments of ablation

* Corresponding author. Tel.: +1-510-642-0421; fax: +1-510-643-9685

E-mail address: debonnel@nuc.berkeley.edu (C.S. Debonnel).

46 and venting phenomena have been given by Chen
47 [1], Liu [2], Scott [3] and Jantzen [4], but recent
48 improvements in the liquid pocket design require a
49 new investigation to evaluate how effectively the
50 current hybrid HYLIFE II design protects the
51 beam tubes and ultimately the final focus magnets.
52 A detailed assessment of the gas dynamics in a
53 beam tube has never been done before and an
54 outline of the relevant physics is given here, along
55 with the required improvements in numerical
56 modelling that should be made to assess the
57 venting through the beam tubes. Calculations are
58 also presented for the impulse loads delivered to
59 target facing surfaces by X-ray ablation and
60 pocket pressurization, since these loads are im-
61 portant in assessing the liquid response and the
62 effectiveness of pocket regeneration.

63 2. The target chamber

64 2.1. Numerical modelling of the target chamber

65 The Berkeley CFD TSUNAMI code (Chen et
66 al. [5]) has been revised and extended to model the
67 hybrid HYLIFE chamber (Debonnel et al. [6]). It
68 solves the one-dimensional Euler's equations for
69 compressible flow using the Godunov's method as
70 refined by Colella et al. (see [6] and the references
71 therein). Operator splitting is used for two-dimen-
72 sional calculations.

73 The fusion pellet and holhraum are modelled as
74 a spherical source emitting a specified amount of
75 debris and a given yield. The target is assumed to
76 radiate X-rays at a single blackbody temperature.
77 The fraction of energy that goes into the X-rays
78 and the one that goes into the debris are specified.
79 The amount of ablated pocket material is assessed
80 via the cohesive energy model. The X-ray energy
81 deposited in target-facing liquid surfaces is com-
82 puted using photon absorption cross sections, and
83 vaporization is assumed to occur down to the
84 depth where the energy density reaches the cohe-
85 sive energy. The vaporization is assumed to be
86 instantaneous and is imposed as an initial condi-
87 tion for the subsequent gas dynamics.

88 Due to their large inertia, the liquid structures
89 are assumed to remain stationary during the entire

90 venting process. During a TSUNAMI calculation,
91 the liquid jets do not have the time to move
92 notably and the disruption of the jets due to
93 neutron isochoric heating or pressure build-up
94 also happen sufficiently slowly that it does not
95 alter the vent paths geometry, except where the
96 venting gaps are very small. Boundary conditions
97 are open at the location of the beam tubes and the
98 condensing area. (The injected droplets are as-
99 sumed to condense all of the mass that flows onto
100 them.) The boundary condition is closed at the
101 surface of the thick-liquid structures. Convective
102 transport is assumed to predominate over heat
103 transfer effects at these boundaries. Most of the
104 condensation is expected to occur on droplets in
105 the condensing region.

2.2. Study cases 106

107 This analysis considers a two-sided illumination
108 by a 9×9 square beam array. Not all of the
109 positions in the 9×9 lattice are necessarily filled
110 with actual beams. In particular, corner apertures,
111 and likely center ones, are left empty to create a
112 more cylindrically symmetric beam pattern. The
113 9×9 pocket geometry has been idealized (see Fig.
114 1), so that it can be modelled with a two-
115 dimensional code. The hybrid target chamber has
116 been assumed to be axially symmetric around the
117 direction of the target injection path.

118 A real gas equation of state adapted from
119 Chen's work [1] has been employed. The target is
120 assumed to be a sphere of 10 g with a typical yield
121 of 450 MJ, 4% of which is given to the debris, 25%
122 to the X-rays, and the remainder removed by
123 neutrons.

124 At the very beginning, the vapor in the chamber
125 is quiescent with a pressure corresponding to the
126 saturation one in equilibrium with the liquid at 873
127 K, where its density is equal to $1.6 \times 10^{-7} \text{ kg m}^{-3}$,
128 as prescribed by Olander et al. [7]. While the
129 equilibrium vapor is composed primarily of the
130 more volatile component BeF_2 , in these TSU-
131 NAMI calculations, the gas is assumed to have
132 the same stoichiometric composition as flibe, and
133 mass transfer effects are neglected. This assump-
134 tion is reasonable because the mass of the initial
135 equilibrium vapor is small compared to the mass

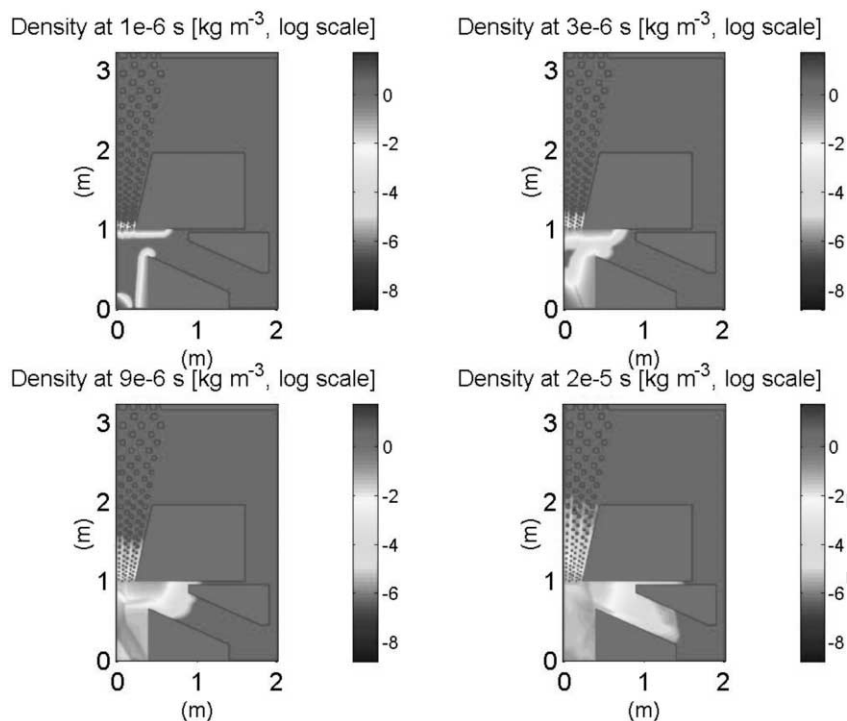


Fig. 1. Density contour plots at various times. The density of the liquid and solid structures is arbitrarily low.

136 of ablation debris. However, at long times (after a
 137 few tens of milliseconds), as the chamber vapor
 138 approaches equilibrium conditions before the next
 139 shot, LiF and NaF will condense preferentially,
 140 modifying the composition in the vapor phase.

141 2.3. Results

142 The X-rays vaporize 0.56 kg of flibe. For the
 143 standard 9×9 axially symmetric hybrid case (Fig.
 144 1), an integrated mass flux of 1.8 g m^{-2} has been
 145 computed after 1 ms at the entrance of a beam
 146 tube on the target injection axis (Fig. 2). (In other
 147 words, $14 \mu\text{g}$ of debris enters the centerline tube
 148 per shot.) The integrated energy flux after 1 ms is
 149 3.2 MJ m^{-2} (Fig. 3). (This corresponds to 25 kJ
 150 entering the centerline tube per shot.) Off-axis,
 151 mass and energy fluxes drop. These two-dimen-
 152 sional TSUNAMI calculations predict a reduction
 153 by two orders of magnitude for the fluxes at the
 154 entrance of the most off-axis tubes. These results
 155 were obtained for a condensing area of 79 m^2 and

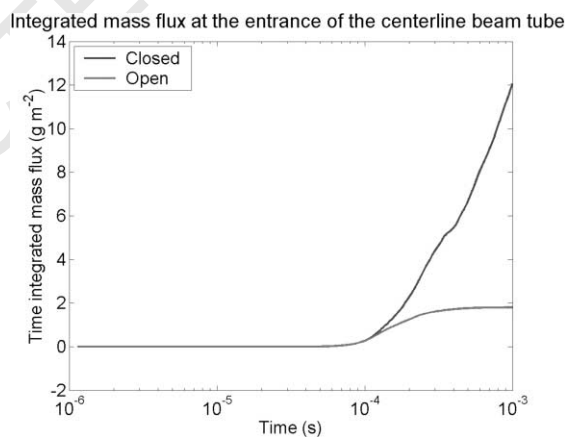


Fig. 2. Integrated mass flux.

are dependent on the area of the chamber wall that
 is assumed to open into condensing regions. If the
 chamber wall has no condenser opening, the
 integrated mass flux rises to 8.0 g m^{-2} in 1 ms
 and the integrated energy flux is 12 MJ m^{-2} .

156
 157
 158
 159
 160

Integrated energy flux at the entrance of the centerline beam tube

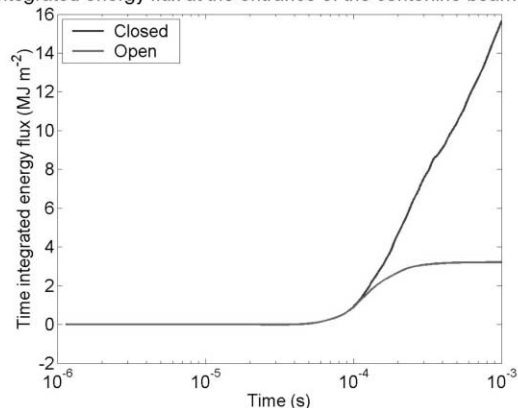


Fig. 3. Integrated energy flux.

161 The impulse load to the target-facing liquid
 162 structures is estimated to be 1.4 kPa s^{-1} (Fig. 4).
 163 The first rise is due to the expansion of the
 164 ablation debris, which exercise pressure work on
 165 the jets. The pocket pressurization causes the
 166 second rise in impulse load. Numerical conver-
 167 gence has been investigated by decreasing the
 168 Courant–Friedrichs–Lewy (CFL) number and
 169 the mesh size. With a smaller CFL number, the
 170 tracking of the shock waves is improved but the
 171 results are similar. Decreasing the size of the mesh
 172 did not change the results significantly.

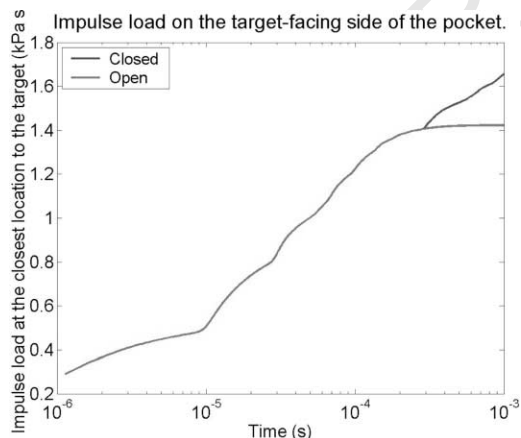


Fig. 4. Impulse load.

3. The beam tubes

173

3.1. Flibe versus flinabe

174

Controlling the pressure in the beam tube 175
 requires the careful choice of the thick liquid 176
 composition used and its temperature. Neutronics 177
 and the effectiveness of magnet shielding, as well 178
 as thermal hydraulics properties must be taken 179
 into account. The blanket must also breed the 180
 tritium fuel required by traditional DT targets. 181
 HYLIFE I was designed to use liquid lithium. 182
 HYLIFE II uses the molten salt flibe instead, to 183
 decrease the fire hazard and improve neutron 184
 shielding effectiveness, while preserving tritium 185
 breeding and good neutronics properties. How- 186
 ever, the melting temperature and vapor pressure 187
 of flibe are a concern. An approach to reducing the 188
 melting temperature of flibe substantially has been 189
 identified. Some of the lithium fluoride (LiF) may 190
 be replaced by sodium fluoride (NaF). 191

Adding roughly 30% NaF to flibe, creating 192
 “flinabe”, depresses the melting temperature 193
 from 733 K to less than 673 K. When used at 194
 temperatures below the melting temperature of 195
 flibe, this ternary salt mixture has a much lower 196
 equilibrium vapor pressure (roughly estimated to 197
 be 0.1 mPa at 713 K) and density (around 10^{16} 198
 m^{-3}), which makes it compatible for use in heavy- 199
 ion beam lines. Adding up to 25% NaF is not 200
 expected to decrease the breeding factor enough to 201
 cause concern, as estimated by Latkowski [8]. 202
 Flinabe might therefore be used instead of flibe 203
 in the target chamber as well as in the beam tubes, 204
 simplifying the overall hydraulics design by having 205
 one coolant loop instead of two. 206

3.2. Flinabe: the panacea?

207

As shown in Fig. 5, one or two vortices would 208
 be used. Such vortices have been demonstrated to 209
 be feasible in scaled water experiments [9]. One 210
 vortex would coat the inside of the beam tube up 211
 to the neutralization area, and possibly a second 212
 vortex would extend from there through the final 213
 focus magnet region. The vapor pressure of flinabe 214
 is sufficiently low that it can be used to cover the 215
 inside of the beam tubes in the final focus magnets 216

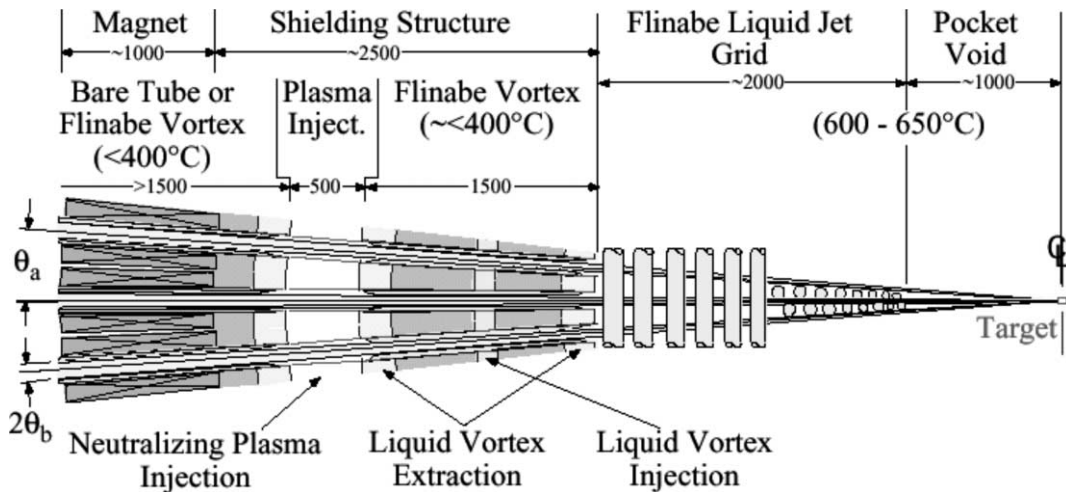


Fig. 5. Beam-line schematic. Lengths are in mm. θ_a is the array half-angle, θ_b the beam half-angle.

region. An effective coating of the beam tubes may alleviate the burden of using shutters to protect the beam tubes.

However, the electrical breakdown properties of flinabe liquid surfaces remain to be investigated. A high resistivity may induce an electrical breakdown during the passage of the beams upstream of the neutralization point, where the high space charge of the beams creates high electrical fields. For an unneutralized 4-kA beam, moving at 20% of the speed of light, and a pipe radius of 5 cm, the steady electric field is 200 kV cm^{-1} . This is substantially more than the 20 kV cm^{-1} typically required to generate voltage breakdown with insulators. However the liquid flinabe will likely have different characteristics than solid insulators. In particular flinabe will have much lower absorbed gas concentrations than typical solid insulators: Absorbed gas is actually believed to generate the initial electrons required for surface breakdown and flashover in most insulators. The short duration of a beam pulse may help to alleviate this flashover concern too.

3.3. Qualitative gas dynamics in the beam tubes

The first puffs of ablation debris will be hot enough to vaporize some flinabe from the surface of the beam tube vortex. Along the beam tubes, the gas will cool by heat transfer and by mixing

with evaporated vortex liquid, and ultimately will condense. An efficient thick-liquid protection scheme should cause all the ablation debris to condense before the final-focus region or would otherwise prevent the gas from reaching the final-focus magnet region.

A detailed assessment of the mass flux at the entrance of the beam lines will require the consideration of three-dimensional effects, as well as a refined real gas equation of state and treatment of evaporation and condensation on liquid surfaces in the jet array. The current code and computing power do not allow the concurrent simulation of the target chamber and beam tubes. Runs for the beam tubes will have to be performed separately, using the results from target chambers simulations as inlet conditions. Therefore, a time-dependent boundary condition capability will have to be implemented into TSUNAMI.

4. Conclusion

Mass and energy fluxes at the entrance of the centerline beam tube have been estimated. The chamber volume and condenser area are key components in controlling the mass flux at the entrance of the beam tubes, since it determines how rapidly the average gas pressure drops in the chamber. The hot puff that originally enters the

245
246
247
248
249
250
251
252
253
254
255
256
257
258
259
260
261
262
263

264

265
266
267
268
269
270
271

ARTICLE IN PRESS

6

C.S. Debonnel et al. / Fusion Engineering and Design 00 (2002) 1–6

272 beam tubes is expected to vaporize some of the
273 vortex liquid, whereas condensation should be a
274 key process to keep the pressure and density low
275 further up in the beam tubes.

276 Acknowledgements

277 This work was performed under the auspices of
278 the US Office of Fusion Energy Science under
279 contract DE-FG03-97ER5441. Fruitful conversa-
280 tions with Dr Yu from LBNL are gratefully
281 acknowledged.

282 References

283 [1] X.M. Chen, A Study of Thermal Hydraulic and Kinetic
284 Phenomena in HYLIFE-II—An Inertial Confinement Fu-
285 sion Reactor, Ph.D. thesis, University of California at
286 Berkeley, 1992.
310

[2] J.C. Liu, Experimental and Numerical Investigation of 287
Shock Wave Propagation Through Complex Geometry, 288
Gas Continuous, Two-Phase Media, Ph.D. thesis, Univer- 289
sity of California at Berkeley, 1993. 290
[3] J.M. Scott, X-Ray Ablated Plumes in Inertial Confinement 291
Fusion Reactors, Ph.D. thesis, University of California at 292
Berkeley, 1998. 293
[4] C.A. Jantzen, Gas Dynamics and Radiative Heat Transfer 294
in IFE Chambers with Emphasis on the HYLIFE-II Design, 295
Ph.D. thesis, University of California at Berkeley, 2000. 296
[5] X.M. Chen et al., Code Description Document, TSUNAMI 297
2.6: A Program for Predicting Gas Dynamics in Inertial 298
Fusion Energy Target Chambers, Nuclear Engineering 299
Department, University of California at Berkeley, 1998. 300
[6] C.S. Debonnel et al., Code Description for TSUNAMI 301
2.8.2, personal document, 2002. 302
[7] D.R. Olander, G. Fukuda, C.F. Baes, Equilibrium pressures 303
over BeF₂/LiF (flibe) molten mixtures, *Fusion Science and* 304
Technology 41–2 (2002) 141–150. 305
[8] J.F. Latkowski, personal communication, 2001. 306
[9] S.J. Pemberton, Thick Liquid Protection in Inertial Fusion 307
Power Plants, Ph.D. thesis, University of California at 308
Berkeley, 2002. 309

UNCORRECTED PROOF